



A holistic review on the synthesis techniques of spinel structured lithium cobalt manganese tetroxide

Chee Wayne TAN¹, Zul Hilmi CHE DAUD^{2,*}, Zainab ASUS², Mohd Hasbullah IDRIS¹, Izhari Izmi MAZALI¹, Mohd Ibthisham ARDANI¹, and Mohd Kameil ABDUL HAMID²

¹ School of Mechanical Engineering, Faculty of Engineering, Universiti Teknologi Malaysia, 81310 Johor Bahru, Johor, Malaysia

² Automotive Development Centre, School of Mechanical Engineering, Faculty of Engineering, Universiti Teknologi Malaysia, 81310 Johor Bahru, Johor, Malaysia

*Corresponding author e-mail: hilmi@mail.fkm.utm.my

Received date:

16 August 2022

Revised date:

30 September 2022

Accepted date:

2 October 2022

Keywords:

LiCoMnO₄ cathode;
Solid-state;
Sol-gel;
Flux;
Hydrothermal

Abstract

Spinel structured lithium cobalt manganese tetroxide (LiCoMnO₄) which exhibit unrivalled reduction potential of 5.3V (vs. Li⁰ | Li⁺) was identified to be one of the potential cathode candidates for next generation lithium-ion batteries offering high voltage output and energy density. The focal point of this article is to holistically review relevant techniques established for the synthesis of LiCoMnO₄ compound, particularly solid-state reaction, sol-gel synthesis, flux method and hydrothermal technology. Electrochemical performances of lithium cobalt manganese tetroxide (LiCoMnO₄) synthesised via the four distinctive approaches as well as the critical process parameters will be compared and scrutinised. Adversities associated with deoxygenation in the course of synthesis process at high temperature and proposed countermeasure via fluorine-substitution will also be discussed.

1. Introduction

The approach of deriving energy through the combustion of fossil fuels had enabled the humankind to achieve unprecedented transformation on various aspects of development over the past century, but also simultaneously instigated global air pollution that accounts for climate change [1] as well as alarming health related issues involving more than three million cases of premature death annually [2]. Anthropogenic air pollution in urban areas in particular had been identified to predominantly originated from land transportation sector especially emission in the form of particulate matters as well as greenhouse gases [3].

Various sustainable alternatives on renewable energy such as photovoltaic, wind turbine, hydrokinetic, hydrogen fuel cell and geothermal have been developed and implemented exponentially in conjunction with power-to-X concept, dispatchable power generation as well as advanced energy storage technology [4-14] in recent years as parts of the global efforts to gradually decommission the usage of fossil fuels and reduce carbon footprints in order to overcome air pollution. Despite facing great obstacles, strategic measures such as incentivise the usage of electric vehicles, impose strict emission standard [15] and eventually legislative enforcement to ban the sales of gasoline as well as diesel powered vehicle had been initiated by several developed nations with the ultimate intention to completely phase out fossil fuels from land transportation sector by 2040 [15,16].

The breakthrough of intercalation technology with graphite anode coupled with the discovery lithium cobalt oxide (LiCoO₂) cathode in early 1990s had led to the emergence of practical rechargeable lithium-ion energy storage system that display relatively higher energy density, voltage output, tiny memory effect as well as low self-discharge rate as compared against its predecessors [17]. Lithium-ion battery technology which had undergone maturation phase and refined through the adoption in diversifying non-stationary applications along with rapid development on cutting-edge electric motor technology as well as state-of-the-art electronic components for efficient control systems triggered immense market interest for zero emission electric powered vehicles [18].

Nevertheless, it was reported that scarcity of electric vehicle charging infrastructure in majority of the market regions at the present time induced range anxiety for majority of the consumers [16]. The United States Department of Energy and Advanced Battery Consortium estimated that privately owned electric vehicle should attain driving range of 500 km which corresponds to approximately 235 Wh.kg⁻¹ and 500 Wh.L⁻¹ at battery pack level or 350 Wh.kg⁻¹ and 750 Wh.L⁻¹ at cell level in order for zero emission locomotive technology to achieve tipping point for mass market penetration [19].

Since the energy per unit mass or volume of electrochemical systems are primarily governed by the voltage output, V as well as quantity of electrons charge per unit mass or volume, Q as shown in equation (1) or alternatively represented by equation (2), increasing the redox

potential between electrodes and enriching the electrodes with lithium content will effectively improve the energy density [20]. The focal point of this article is to holistically review the synthesis methodology of lithium cobalt manganese tetroxide (LiCoMnO_4) that display high reduction potential to elevate the voltage output of lithium-ion batteries.

$$E = VQ \quad (1)$$

$$E = I \int_0^t V dt \quad (2)$$

2. The fundamentals of battery electrochemistry

The term battery in the context of power electronics is defined as an assembly of two or more electrochemical cells that function simultaneously as an integrated reservoir for energy storage, primarily in the form of chemical system which can be directly convertible into electricity [21]. Each of the fundamental unit electrochemical cells within electrical battery may be considered as isolated systems from thermodynamic perspective and essentially constructed of active anode, cathode and electrolyte as well as current collectors and ionically permeable separator as shown in Figure 1 [18,22,23].

The kinetic operation of electrochemical system is mainly governed by interface reaction between the electrodes and electrolyte [24]. The chemical reaction in primary electrochemical cells is irreversible, therefore can only be discharged once and must be entirely replaced when the supply of reactants in the device completely depleted since they are not able to be electrically refilled [18]. The chemical reaction in secondary cells used in rechargeable batteries on the other hand are reversible as electric current were applied to the device and regenerates the original chemical reactants, allowing the device to be repetitively discharged and recharged for a finite cycle [17].

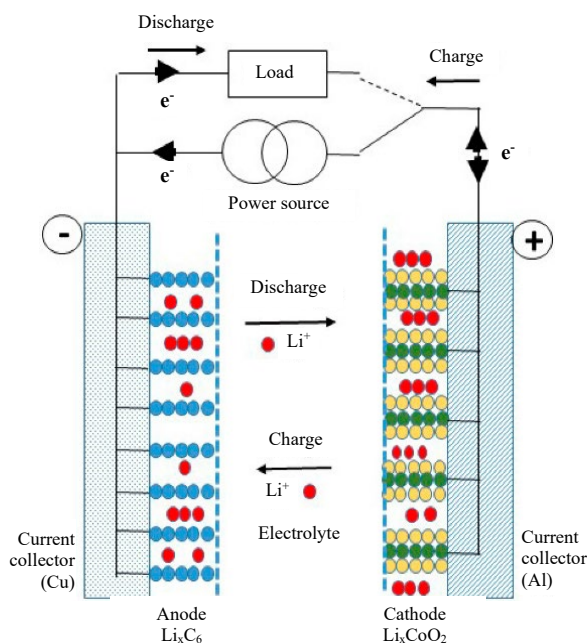


Figure 1. Schematic Diagram of Electrochemical Cell [23] Copyright permission for reuse granted by publisher under Creative Common CC-BY License.

Rechargeable batteries designed for high voltage output and energy density such as lithium-ion electrochemical system shall ideally be constructed of anode materials that exhibit low oxidation potential, $E_{\text{oxidation}}$ and paired with cathode compounds that possess high reduction potential, $E_{\text{reduction}}$ relative to lithium metal [20,25]. Oxidation will take place on the anode, while reduction will occur on the cathode during discharge and vice versa during charging cycle. The electromotive force or theoretical discharge voltage, E_0 of the electrochemical system may be computed via equation 3 [26].

$$E_0 = E_{\text{reduction(cathode)}} - E_{\text{oxidation(anode)}} \quad (3)$$

2.1 Anodes

Anodes which are also alternatively known as negative electrode in the context of electrical battery or electrochemical cell during discharge are commonly made up of materials that can be easily oxidised and readily yield electrons to form ions [18]. Lithium metal that displays inherently low redox potential have been widely adopted as the anode for primary batteries due to the high nominal output voltage as well as remarkable energy and power density, but never been successfully integrated into pragmatic rechargeable electrochemical systems due to the tendency for the formation of dendrites on the anode during charging cycle which potentially induce short circuit and thermal runaway [27].

Rechargeable lithium-ion batteries which have been adopted in diversifying applications ranging from portable electronic devices to telecommunication, military, aerospace and automotive sectors were constructed of lithiated graphite anode which exhibit the forte in discontinuing the growth of dendrites formed in the course recharge cycles through dissolution by electric current during subsequent discharge cycles [28]. Besides featuring rechargeability, lithium-ion batteries also display relatively high energy and power density, tiny memory effect as well as slow self-discharge rate [18,29].

Nevertheless, the net loss of active anode material in lithium-ion battery with charge and discharge cycle over time will however led to performance degradation [30]. Lithium-ion batteries also possess relatively narrow operating temperature range, as discharge in high temperature may compromise in term of safety factor due to the presence of flammable and volatile electrolyte, while storage at low temperature may induce self-draining due to elevated internal resistance [31]. The overall regulated charging rate of lithium-ion battery which are relatively spun-out when compared against the conventional refuelling method used in automobile powered by internal combustion engines have also been identified to be among the main hindrances for global widespread adoption of electric vehicle [32].

Lithium titanate have been developed as one of the potentially viable anode candidates for the adoption of fast charging battery systems in electric vehicle, offering relatively wide range of operating temperature, high durability, coulombic efficiency as well as capable of delivering high rate and power capability [33,34]. The performance of lithium titanate battery at the present time however was compromised by relatively low nominal output voltage (-30% as compared against standard graphite electrode in lithium-ion battery system) when paired with commercially available cathode compounds [35,36].

2.2 Cathodes

Cathodes which are also alternatively known as positive electrodes in the context of electrical battery are commonly made up of materials that can be easily reduced and readily accept electrons during discharge [18]. Direct current (DC) will be instantaneously produced as circuit connection is complete and the outgoing electrons donated by the anode flow through the load of external circuit accepted by the cathode [18].

The insertion and extraction process of guests into and out of the host vacancies which is also termed as intercalation mechanism in the context of electrochemical systems are primarily governed by the molecular geometric lattice frameworks as well as ionic diffusion passageways of electrodes [26]. Positive electrodes for rechargeable lithium-ion batteries may be classified into three major categories, namely the olivine structure that display one-dimensional (1D) ionic diffusion channel, layered two-dimensional (2D) structure by which transition metal cations occupy alternate lattices between the anions and lithium ions intercalated into the empty interlayers as well as three-dimensional (3D) spinel structured compounds with the presence of interstitial sites and pathways that facilitate ionic diffusion [26].

The concept of non-aqueous rechargeable electrochemical system was first demonstrated in the early of 1972 [37] with initial prototypes constructed of binary system transition metal chalcogenides cathode compound specifically titanium disulphide (TiS_2) that display 2D layered structure [38,39]. It was reported that presence of transition metal enhanced the overall chemical stability of electrodes, thereby reducing the tendency for the occurrence of alloying reaction especially with lithium or sodium which enable practical repetition of charge and discharge cycle while maintaining good electron conductivity via metallic nanonetwork [40].

Following the scientific breakthrough and successful patents filed under Bell Telephone Laboratories Inc., several layered structure binary system transition metal based cathode compounds such as tungsten sulphide (WS_2), molybdenum oxide (MoO_3) as well as vanadium oxide (V_2O_5) were subsequently developed and investigated [26]. The discovery of mixed-valence quasi-layered lithium trivanadate (LiV_3O_8) which is also known as lithia-stabilised vanadium oxide that display remarkable resistance towards chemical degradation during intercalation and de-intercalation eventually steered the research focal point towards relatively complex ternary system 2D layered structure cathode compounds [26].

Lithium cobalt oxide (LiCoO_2), being first independently developed by Professor John Bannister Goodenough and further scaled up for mass production as well as commercialisation in collaboration with Sony Corporation was identified to be the most prominent cathode compound that truly enabled rechargeable lithium-ion battery technology to reach its tipping point in the early of 1990s and still remained to be one of the most dominant category of compounds in the global energy storage market until present [38]. It was reported that LiCoO_2 display relatively high theoretical gravimetric and volumetric capacity at $274 \text{ mAh}\cdot\text{g}^{-1}$ and $1363 \text{ mAh}\cdot\text{cm}^{-3}$ respectively [26,41].

Besides, LiCoO_2 also display stable cycling performance, slow self-discharge which translate to longer shelf-life and capable of delivering high discharge voltage as compared to its predecessors [41]. Nevertheless, high cost, low thermal stability and fast capacity fade at high current rates or during deep cycle discharge was identified

to be the main drawbacks possessed by LiCoO_2 [38]. Moreover, empirical experiment and field test revealed that the loss of oxygen from the layered ternary system compound over charge and discharge cycle resulted in capacity fading due to reduction in lithium content on the cathode corresponding to the negated intercalation reaction, therefore can only practically deliver approximately $140 \text{ mAh}\cdot\text{g}^{-1}$ [41].

Several isostructural derivatives which often being abbreviated as LiM_xO_y were subsequently developed to address performance limitations, cost effectiveness and long-term sustainability issues faced by LiCoO_2 as the global demand for lithium-ion batteries increases [26]. Lithium nickel oxide (LiNiO_2) exhibit better cycling stability [42] as well as capable of delivering higher magnitude of practical capacity and operating voltage as compared against LiCoO_2 [41,43], while lithium manganese oxide (LiMnO_2) is cost effective, environmentally benign and offer higher safety factor due to better thermodynamic stability especially with predomination of orthorhombic crystal over monoclinic lattice [38,44].

Nevertheless, it was reported the existing processing techniques established for the synthesis of LiNiO_2 require the reactants to exposed to high temperature that often resulted in non-stoichiometric composition which in turn led to partially disordered cation distribution at the lithium sites [41,43]. LiMnO_2 also tends to lose capacity drastically as a result of relatively high volumetric expansion and structural strain as well as Jahn-Teller distortion that promote oxidation of as Mn^{3+} into Mn^{4+} , causing phase transformation of monoclinic into regular hexagonal structure over charge and discharge cycles [41,43]. Ternary system phase diagram involving LiCoO_2 , LiNiO_2 and LiMnO_2 as illustrated in Figure 2 [23] was investigated as early as 1991 [45] to formulate all-encompassing cathode compound with layered structure that possess all the merits while off-setting their drawbacks [38,46]. After more than a decade of development, lithium nickel manganese cobalt oxide, LiNiMnCoO_2 was commercialised in 2008 to unleash the potential of lithium-ion batteries for the adoption in medical devices, industrial power tools as well as electric vehicles [47].

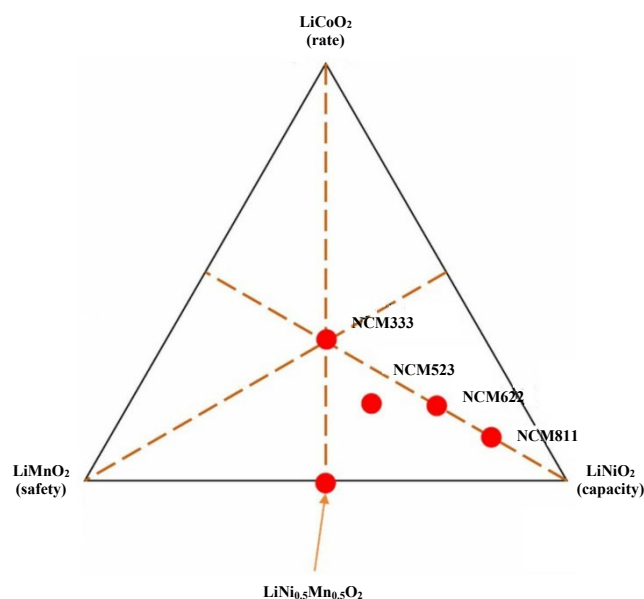


Figure 2. LiCoO_2 - LiNiO_2 - LiMnO_2 Phase Diagram [46] Copyright permission for non-commercial reuse, distribution and reproduction granted by publisher.

While it is common for the transitional metals within $\text{LiNi}_x\text{Mn}_y\text{Co}_z\text{O}_2$ compounds, where $x + y + z = 1$ to be empirically formulated in the ratio of 1:1:1, wide variety of isostructural derivatives can be precisely customised in order to meet the specific functional requirement of diversifying applications [23]. Besides, elements beyond the group of transition metals such as boron, aluminium and gallium may also be introduced for functional purposes, for instance lithium nickel cobalt aluminium oxide (LiNiCoAlO_2) cathode formulated to deliver higher specific energy for electric powertrain [48]. Olivine structured polyanionic lithium transitional metal phosphates, LiMPO_4 and lithium transitional metal silicates, LiMSiO_4 , which display one dimensional order have also been developed as they are commonly bonded by van der Waals force that can be easily overcome to facilitate intercalation reactions [26,49].

Lithium iron phosphate (LiFePO_4) was reported display good thermal stability, tolerant to overcharging as well as capable of delivering significantly higher specific power, nevertheless in general exhibit lower capacity, redox potential and substandard energy density, hence primarily used for stationary energy storage applications [17,38]. Whilst lithium iron silicate (LiFeSiO_4) offering remarkable redox potential of up to 4.8 V (vs. $\text{Li}^0 | \text{Li}^+$), the compound however was discovered to exhibit poor reversibility and unstable electrochemical performance due to relatively high charge transfer resistance [38,41].

Cathode compounds that display lower structural dimensionality order in general are constructed by arrays of molecules affixed together with strong ionic or covalent bonds, where the chains are interlinked by relatively weak van der Waals force that can be easily overcome to allow entry as well as departure of intercalant during charge and discharge cycle which is favourable for the occurrence of intercalation reactions [11]. Nevertheless, the heterogenous reaction occurred within electrochemical cells often induce irreversible alteration to the structure of intercalation compounds as the electrodes are repetitively subjected to oxidation and reduction over time [26].

It was reported that compounds which exhibit complex three-dimensional (3D) spinel structure may also effectively function as intercalation host, provided that interstitial sites are available along with the presence of pathways that facilitate ionic diffusion [11]. Lithium manganese tetroxide (LiMn_2O_4) was identified to be the first spinel structured cathode compound developed to address the drawbacks possessed by the layered and olivine structured cathodes [41].

It was reported that LiMn_2O_4 cathode display redox potential of 4.1 V (vs. $\text{Li}^0 | \text{Li}^+$) with theoretical capacity of $148 \text{ mAh}\cdot\text{g}^{-1}$ [26,41]. Nevertheless, empirical experiment revealed that the inorganic compound merely attained practical capacity of $120 \text{ mAh}\cdot\text{g}^{-1}$ [41]. Moreover, LiMn_2O_4 cathode are susceptible to drastic capacity fading especially when cycled above 60°C [26,41].

Research efforts to elevate the energy density as well as operational voltage of lithium-ion electrochemical system by increasing the redox potential between electrodes had led to the development of three-dimensional spinel structured quaternary system $\text{Li}\Omega_x\text{Mn}_{2-x}\text{O}_4$ compound [50]. The term “ Ω ” represents individual transition metallic element which are commonly positioned on the fourth horizontal row in the periodic table of chemical elements [50].

Lithium cobalt manganese tetroxide (LiCoMnO_4) which exhibit cubic space group $\text{Fd}\bar{3}\text{m}$ spinel crystal structure [51], where the Co^{3+} and Mn^{4+} ions are randomly distributed in the 16d octahedral sites, while

Table 1. Redox Potential of $\text{Li}\Omega_x\text{Mn}_{2-x}\text{O}_4$ Compounds [50].

Ω	Redox potential (vs. $\text{Li}^0 \text{Li}^+$)
Nickel (Ni)	4.7
Chromium (Cr)	4.8
Iron (Fe)	4.9
Cobalt (Co)	5.1

Li^+ ions are located at the 8a tetrahedral sites could attain remarkably high redox potential at 5.1 V proximity (vs. $\text{Li}^0 | \text{Li}^+$) [50,52]. Lithium cobalt manganese tetroxide cathode not only surpassed the performance of its coequal counterparts as shown in Table 1, but also significantly outperformed its predecessors by more than 20% [50,51].

Meanwhile, it was reported that LiCoMnO_4 may attain up to $145 \text{ mAh}\cdot\text{g}^{-1}$ of theoretical specific capacity with fully reversible extraction and insertion of Li^+ ions through the three-dimensional pathways in between the 8a tetrahedral sites and vacant 16d octahedral sites from the spinel crystal lattice [50]. Electrons will be stored by transition metal ions during charging, while removed from the transition metal ions during discharge cycle [52]. Besides, it was also reported that LiCoMnO_4 possessed exceptional dimensional stability, where the cathode subjected to only approximately 0.7% of volumetric change during charge and discharge cycles, hence suggesting the compound to potentially emerge as a viable positive electrode candidate for all-solid-state battery applications [50,53].

LiCoMnO_4 cathode had not been made commercially available in the present time due to unresolved safety hazards especially when paired with lithium intercalated graphite anode and operated above 4.7 V which may induce decomposition of electrolytes and outgassing [52,54]. However, several studies suggested LiCoMnO_4 cathode may potentially be paired with lithium titanate anode which display oxidation potential of 1.55 V (vs. $\text{Li}^+ | \text{Li}^0$) [51] to harvest the benefits of fast charging capability without operating beyond deterrent voltage limit [55].

3. Synthesis of lithium cobalt manganese tetroxide

Whilst scientific research on lithium cobalt manganese tetroxide (LiCoMnO_4) as cathode for energy storage system was instigated as early as 1998, relevant literatures and credible information on the subject up to date still remained scarcely available [51]. Synthesis approach and fabrication methodology of LiCoMnO_4 may directly influence the electrochemical performance of the cathode compound. Various techniques ranging from solid-state reaction, sol-gel synthesis, flux method, as well as hydrothermal technology have been developed and adopted for the synthesis of lithium cobalt manganese tetroxide will be discussed.

3.1 Solid-state reaction

Preliminary research on the synthesis and performance of lithium cobalt manganese tetroxide (LiCoMnO_4) was initiated by Kawai *et al* through solid state reaction technique [56,57]. The lack of consistency in term of process variables as well as precursors used in producing LiCoMnO_4 were perceptible between research laboratories [50]. Kawai *et al* selected reagent grade Li_2CO_3 , MnCO_3 as well as CoO and blended them in stoichiometric ratio prior to mechanical grinding

followed by decarbonation at 650°C for 2 h to remove carbon dioxide [56]. The homogenised mixtures were reacted at 800°C for 72 h with regrinding at intervals followed by annealing at 600°C for another 72 h to recover the oxygen loss induced by firing at high temperature before quenching to room temperature [56].

Kuwata *et al* in 2013 adopted similar approach by selecting similar inorganic compounds as reactants and processing temperature yet with controlled heating rate of 100°C·h⁻¹ as well as reduced the sintering duration at 800°C by 66.67% [58]. Reeves-McLaren *et al* in 2018 however embraced a relatively different approach in the synthesis of LiCoMnO₄ and start by blending stoichiometric proportion of Co(NO₃)₂·6H₂O, Li₂CO₃ (dehydrated under 180°C) as well as (CH₃CO₂)₂Mn·4H₂O followed by grinding of the mixture with agate mortar and pestle before further heated in alumina crucible to remove residual moisture, acetate and nitrates [50]. The pulverised mixture was decarbonated at 650°C for 3 h before furnace temperature was ramped up to operate at 800°C for 45 h with interval re-pulverisation to ensure complete reaction [50]. The resultant compound was further annealed at 500°C for 72 h to optimise the performance by imparting additional oxygen content to the cathode [50].

Despite using different processing approach, both Kuwata *et al* and Reeves-McLaren *et al* obtained comparable x-ray diffraction pattern and near-stoichiometric composition of LiCoMnO₄ with average grain size of less than 0.5 μm. X-ray diffraction analysis result validated that the formation of LiCoMnO₄ without perceptible cationic contamination due the trivial intensity peak detected at [220] corresponding to the crystalline plane producing reflection observed at 31.5° 2θ angle which is highly sensitive to the occupancy at 8a tetrahedral site [50].

Kawai *et al* reported that electrochemical system constructed of lithium anode, LiCoMnO₄ cathode and electrolyte made up of LiPF₆ dissolved in propylene carbonate (PC) attained discharge capacity of 95 mAh·g⁻¹ [56]. Meanwhile, Kuwata *et al* and Reeves *et al* achieved approximately 13% improvement in term of initial discharge capacity at by replacing the organic propylene carbonate solvent with 1:1 ethylene carbonate (EC):dimethyl carbonate (DMC) with no significant deterioration observed over 20 charge and discharge cycles despite using different anode [50,58]. It was also reported that introduction of 2 wt% of 1,3-propane sultone (PS) additive may further increased the discharge capacity and coulombic efficiency of the electrochemical system [50].

The charge and discharge profile of LiCoMnO₄ cathode can be sub-divided into three regimes separated by the two plateaus at 4 V and 5 V region [50,56,58]. The small step observed at 5V proximity was attributed by structural reorganisation of the compound during insertion and deintercalation of lithium ions [50,56,58]. Meanwhile, the plateau corresponding to approximately 4 V vicinity was induced by disproportionated oxygen stoichiometric which is directly correlated to the introduction of additional Mn³⁺ component right before the end of discharge [50,56,58].

Ariyoshi *et. al* in 2017 on the other hand adopted two-step solid state reaction to fabricate LiCoMnO₄ which achieved cell discharge capacity of 120 mAh·g⁻¹ when assembled with lithium anode and discharge at current density of 0.25 A·cm⁻² [53]. The compound was initially reacted at 900°C for 2 h and ultimate undergo oxygenation process at 600°C for 300 h [53].

3.2 Sol-gel reaction

Sol-gel process which involves the conversion of a colloidal suspension (sol) into an integrated 3D polymeric chain network (gel) with submicrometric porosity are often used to produce pulverised ceramics materials due to the capability of the method in producing highly pure particles with uniform morphology and narrow particle size distribution through homogenous mixing of reactants at molecular level [55]. Investigation on the synthesis of LiCoMnO₄ via sol-gel reaction was initiated by Huang *et al* in 2012 with Co(CH₃COO)₂·H₂O, Mn(CH₃COO)₂·4H₂O, LiCH₃COO·H₂O and C₆H₈O₇·H₂O being selected as the reactants [51].

The precursors were comingled at the mass ratio of 19.0:15.5:7.3:58.2 before heated up to 90°C to xerogel state [51]. The xerogel was subsequently heated up to 380°C in a muffle furnace for 10 h before subjected to annealing under oxygen enriched atmosphere at 800°C for 24 h [51].

Analysis from inductive coupled plasma atomic emission spectroscopy revealed that LiCo_{1.09}Mn_{0.91}O₄ compound with average particle size of 0.2 μm was produced through sol-gel reaction [51]. Huang *et al* mapped the charge and discharge correlation between voltage and specific capacity of LiCo_{1.09}Mn_{0.91}O₄ with lithium being set as reference electrode and flooded with 1 mol of LiPF₆ in 1:1 ethylene carbonate (EC):dimethyl carbonate (DMC) electrolyte [51].

It was discovered that the LiCo_{1.09}Mn_{0.91}O₄ cathode compound displayed two voltage plateaus at 5.1 V and 4.9 V during discharge cycle. The cathode compound on the other hand attained merely 60% of the theoretical specific capacity value with average discharge capacity of 87.1 mAh·g⁻¹ recorded within 5 initial charge and discharge cycles [51]. The adverse performance may be induced by excessive aggregation of particles which reduced packing fraction as well as incompatible electrolyte system [51].

3.3 Flux reaction

Exploration on the techniques to synthesise single crystal lithium cobalt manganese tetroxide was inspired by research findings which reported that complex oxide-based cathode systems such as LiNi_{0.5}Mn_{1.5}O₄ with monocrystalline morphology that demonstrated excellent rate capability and cycling performance [59]. It was reported that Hamada *et al* for the first time attempted the synthesis of single crystal LiCoMnO₄ compound via flux technique in 2016 with MnCl₂, CoCl₂ and LiOH·H₂O being used as precursors [59].

MnCl₂ and CoCl₂ were first blended at nominal atomic ratio of Co:Mn = 1:1 before manually grounded with agate mortar and pestle in dry air. Lithium hydroxide monohydrate (LiOH·H₂O) which serve as self-flux material was added into the mixture at nominal atomic ratio of Mn:Li = 1:1.5 before heated up to 750 °C for 48 h in an alumina crucible [59].

The mixture was gradually cooled to room temperature at the rate of -6°C·h⁻¹ and the resultant compound was separated from the flux by rinsing the mixture with distilled water [59]. Observation via scanning electron microscopy under ×10000 magnification as captured in Figure 3 suggested complete formation of single phase octahedral shaped crystal LiCoMnO₄ that ranges between 1 μm to 3 μm was attained from the flux reaction with no presence of by-products detected [59].

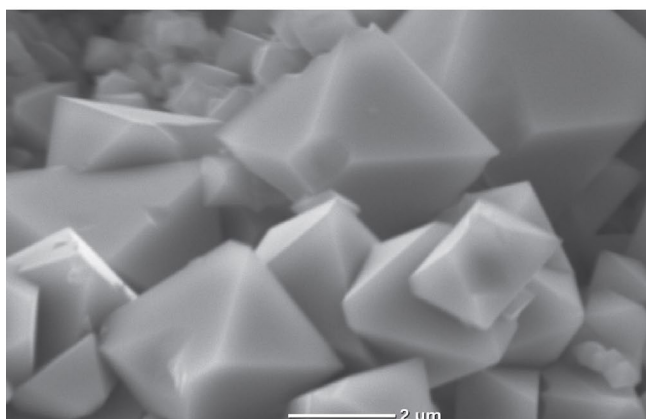


Figure 3. Morphology of LiCoMnO₄ Synthesised via Flux Reaction [59] Copyright permission for reuse and reprint obtained from publisher.

X-ray diffraction analysis also validated that LiCoMnO₄ compound synthesised via flux method exhibit extremely high crystallinity and well indexed to the cubic Fd3m spinel structure with no signs of secondary phase detected [59]. Whilst LiCoMnO₄ with crystal size of 100 μm can be achieved with the adoption of lithium chloride (LiCl) as fluxing agent, however the resultant compound is susceptible to the loss of lithium and accompanied by the presence of secondary phase of Li₂MnO₃ [59].

Analysis from x-ray diffraction and inductive coupled plasma atomic emission spectroscopy revealed that near stoichiometric fraction Li_{0.97}CoMn_{1.03}O₄ compound with lattice parameter, $a = 8.0581 \text{ \AA}$, unit cell volume, $V = 523.240 \text{ \AA}^3$ and number of atoms per unit cell, $Z = 8$ was yielded from the flux reaction [59]. Rietveld refinement performed by Hamada *et al* on from x-ray diffraction (XRD) pattern based on initial structure model of [Li_{1-x}Co_x]_{8a}[Co_{1-x}MnLi_x]_{16d}O₄ with space group Fd-3m (No. 227) attained unweighted profile R-factor, $R_p = 11.1\%$ and weighted profile R-factor, $R_{wp} = 16.9\%$, expected R-factor, $R_e = 12.25\%$ with fit indicator, $S = 1.38$ [59].

It was reported that LiCoMnO₄ synthesised via flux reaction attained 74% of the theoretical specific capacity value with average discharge capacity of 107 mAh.g⁻¹ recorded during initial charge and discharge cycles with three notable voltage plateaus observed at 5.1 V, 4.9 V and 3.9 V vicinity [59]. It was deduced that the two higher peaks at 5 V region were attributed by redox reaction of Co³⁺/Co⁴⁺, while the peak at 3.9 V corresponds to the redox reaction of Mn³⁺/Mn⁴⁺ [59,60].

3.4 Hydrothermal reaction

Inorganic compounds are commonly synthesised through physical chemistry reaction particularly via hydrothermal technique which offer to fast reaction kinetics as well as accompanied by various advantages such as high phase purity, narrow particle size distribution, high crystallinity, environmentally benign and requires significantly lower post-calcination temperature [55]. Besides, hydrothermal reaction also offer cost effectiveness and versatility as the particle size and morphology of the synthesised compounds may be effectively controlled by manipulation of the reaction parameters, while laboratory facilities may be easily scaled up for mass production [55].

The synthesis of lithium cobalt manganese tetroxide via hydrothermal approach was first reported in 2016 where MnSO₄·H₂O ($\geq 99\%$), CoSO₄·H₂O ($\geq 98.5\%$) and (NH₄)₂S₂O₈ were being utilised as the precursors [61]. 0.005 M of MnSO₄·H₂O, 0.005 M of CoSO₄·H₂O as well as 0.0075 M of (NH₄)₂S₂O₈ were added into a 100 mL capacity Teflon container containing 20 mL of deionised water [61]. Meanwhile, LiOH·H₂O ($\geq 98\%$) pre-dissolved in 30 mL of deionised water was gradually introduced into the solution via titration to the target concentration before the container was transferred to a stainless steel autoclave, properly sealed and heated up to 220°C for 22 h [61].

The resultant precipitated compound was separated from solvents by filter mesh, followed by rinsing under running deionised water and dehydrated at 120°C for 24 h before subjected to heat treatment ranging between 550°C to 750°C [61]. Composition of the resultant products was reported to directly correlated to the concentration of LiOH controlled in the course of hydrothermal reaction [61]. You *et al* pin-pointed that the ideal LiOH concentration for the formation of LiCoMnO₄ phase during hydrothermal reaction narrowly ranges between 1.2 M to 1.35 M [61].

It was discovered that in relatively low LiOH concentration condition (0.9 M to 1.1 M), the resultant LiCoMnO₄ compound synthesised via hydrothermal reaction are dominated by the presence of impurity phases particularly LiMn₂O₄, Co₃O₄ and Mn₃O₄ [61]. Meanwhile, the synthesis of LiCoMnO₄ via hydrothermal process in LiOH concentration higher than 1.5 M on the other hand resulted in the formation of excessive secondary phase Li₂MnO₃ [61]. Nonetheless, initial hydrothermal reaction with optimised LiOH concentration only yields LiCoMnO₄ phase of not more than 50% from the overall product formed, while subsequent heat treatment process is crucial in promoting the formation of primary phase [61].

The initial particle size of LiCoMnO₄ synthesised via hydrothermal process generally falls at 0.02 μm proximity before subjected to heat treatment [61]. It was inferred that heat treatment may effectively promote the crystal growth of LiCoMnO₄, where annealing at 750°C may increase the crystallite size up to the range of 0.08 μm to 0.15 μm [61]. The electrochemical cell which were charged and discharged in controlled environment at 27°C were reported to be capable of delivering specific capacity of 91.6 mAh.g⁻¹ [61].

4. Discussion

Collective literature review on various methodology for the synthesis of lithium cobalt manganese tetroxide conjectured the feasibility of fabricating cathode compound with redox potential beyond 5.0 V (vs. Li⁰ | Li⁺) [51,53,56,58,61-63]. Meanwhile, electrochemical cells constructed with lithium cobalt manganese tetroxide cathode synthesised via the four approaches attained relatively similar performance discharge capacity as shown in Figure 4.

It can be observed from Figure 5 and Figure 6 that lithium cobalt manganese tetroxide cathode synthesised via solid-state reaction requires comparatively higher temperature and longer duration, which translate to the highest energy consumption among the four synthesis techniques. Sol-gel technique and flux reaction adopt relatively similar synthesis duration and temperature and resulted in comparable discharge capacity.

Discharge capacity of electrochemical cell constructed of LiCoMnO₄ cathode

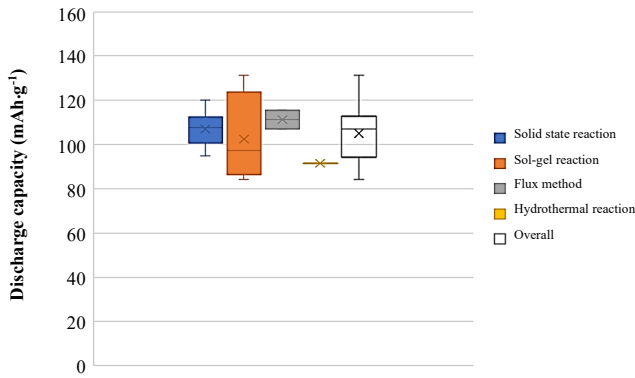


Figure 4. Comparison on Discharge Capacity of LiCoMnO₄ Cathode.

Peak temperature subjected to LiCoMnO₄ during synthesis process

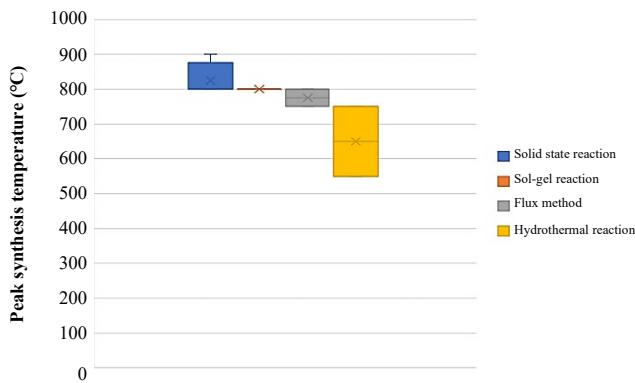


Figure 5. Comparison on Peak Synthesis Temperature of LiCoMnO₄

Total duration required for the synthesis of LiCoMnO₄

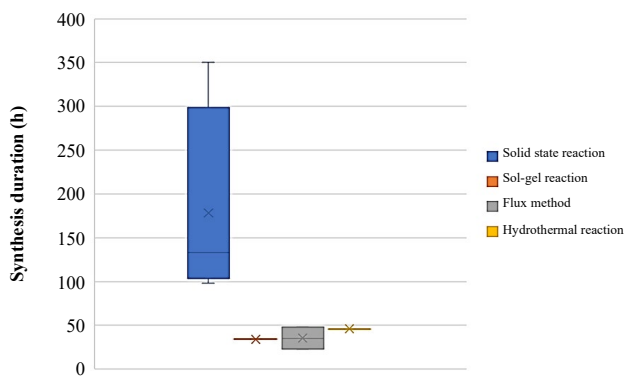


Figure 6. Comparison on Synthesis Duration of LiCoMnO₄

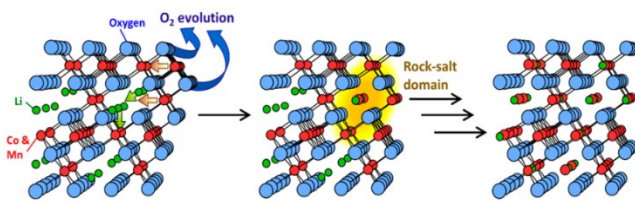


Figure 7. Deoxygenation Mechanism of LiCoMnO₄ during Heating [64]
Copyright permission granted by publisher for print and electronic formats.

4.1 Deoxygenation mechanisms

It was observed that electrochemical cell constructed of LiCoMnO₄ cathode in general display multiple voltage plateaus during discharge cycles, suggesting the presence of undesirable secondary phases such as Li₂MnO₃, LiMn₂O₄, Co₃O₄ and Mn₃O₄ within the resultant inorganic compound which subsequently compromised on the electrochemical performance [61,63].

It was proposed that LiCoMnO₄ are susceptible to oxygen loss in high temperature, especially above 600°C which potentially induced structural transformation from spinel into oxygen deficient cation disordered rock-salt LiCoMnO₃ phase [63] as illustrated in Figure 7 [64]. The synthesis of LiCoMnO₄ which require relatively lower reaction and calcination or heat treatment temperature may potentially mitigate the issue associated with deoxygenation.

Flux method could accelerate the diffusion mechanism of reactants, thereby requires lower synthesis duration while promote crystalline growth and contribute to resultant compound with high purity level [59]. The approach adopted by Hamada *et al* in 2016 which involved dwelling of the precursor compound at 750°C may also be abated to 600°C or lower to reduce the impact of deoxygenation on the resultant compound.

Limited information collated from various independent research as shown in Table 2 which utilised different experimental settings, particularly reactants, anodes, electrolytes and discharge parameters remains debatable and inconclusive. Research parameters such as reference anode, electrolyte system and cell format shall ideally be standardised between the four synthesis techniques in order to pin-point the optimum process for the synthesis of spinel structured lithium cobalt manganese tetroxide.

4.2 Optimisation via Fluorination

Investigation on the synthesis of fluorinated lithium cobalt manganese tetroxide compound was performed by Windmüller *et al* in 2017 via two-step solid-state reaction with LiOH·H₂O, MnCO₃, Co₃O₄ and LiF being used as precursor [52,66]. The formulated mixture was compressed into pellets to improve ease of handling before subjected to calcination in air at 800°C for 10 h, followed by dwelling at 650°C for another 10 h [52]. The calcinated pellets were crushed and finely pulverised before subjected to annealing at 650°C for 72 h in air to refine the microstructure [52].

It was reported that the diffraction peak intensity at [001] corresponding to the crystalline plane producing reflection observed at 18.4° 2θ angle gradually diminished with the increment of fluorine substituent, hence validated the effectiveness of fluorination in suppressing the formation of Li₂MnO₃ phase [52]. Meanwhile, quantitative phase analysis by Rietveld refinement further reaffirmed the importance of fluorine substituent in mitigating the formation of secondary phases [52,67]. Cyclic voltammetry performed on LiCoMnO₄, LiCoMnO_{3.95}F_{0.05} and LiCoMnO_{3.9}F_{0.1} revealed that all of the synthesised compounds exhibit prominent two step reaction at 4.9 V and 5.1 V (vs. Li⁰ | Li⁺) proximity during charge and discharge cycles, corresponding to the redox reaction of Co^{3+/4+} ions [68].

Table 2. Comparison on the Synthesis Techniques of LiCoMnO₄.

Synthesis technique	Reactants	Process	Electrolyte system	Anode	Current density (mA·cm ⁻²)	Discharge capacity (mAh·g ⁻¹)	Year	References
	LiCO ₃ MnCO ₃ CoO	1. Decarbonation: 650°C (2 h) 2. Solid state reaction: 800°C (72 h) 3. Annealing: 600°C (72 h)	Ionic compound: LiPF ₆ Solvent: • propylene carbonate	Li	0.5	95	1998-1999	[56, 57]
	LiCO ₃ MnCO ₃ CoO	1. Decarbonation: 650°C (2 h) 2. Solid state reaction: 800 (24 h) 3. Annealing: 600°C (72 h)	Ionic compound: LiPF ₆ Solvent: 1:1 • ethylene carbonate • dimethyl carbonate	Li	N/A	107	2013	[58]
	LiOH·H ₂ O CoMn(OH) ₂	1. Solid state reaction: 900°C (2 h) 2. 1st annealing: 700°C (24 h) 3. 2nd annealing: 650°C (24 h) 4. Oxygenation: 600°C (300 h)	Ionic compound: LiPF ₆ Solvent: 3:7 • ethylene carbonate • dimethyl carbonate	Li	0.25	120	2017	[53]
Solid state reaction			Ionic compound: LiPF ₆ Solvent: 1:1 • ethylene carbonate • diethyl carbonate			102.5		
	Co(NO ₃) ₂ ·6H ₂ O Li ₂ CO ₃ (CH ₃ CO ₂) ₂ Mn·4H ₂ O	1. Decarbonation: 650°C (3 h) 2. Solid state reaction: 800°C (45 h) 3. Annealing: 500°C (72 h)	Ionic compound: LiPF ₆ Solvent: 1:1 • ethylene carbonate • dimethyl carbonate	Li ₄ Ti ₅ O ₁₂	N/A	108	2018	[50]
			Ionic compound: LiPF ₆ Solvent: 1:1 • ethylene carbonate • dimethyl carbonate Additive: 2 wt% 1,3-propane sultone			110		
Sol-gel reaction	Co(CH ₃ COO) ₂ ·H ₂ O Mn(CH ₃ COO) ₂ ·4H ₂ O LiCH ₃ COO·H ₂ O C ₆ H ₈ O ₇ ·H ₂ O	1. Sol-gel formation: 90°C 2. Xerogel reaction: 380°C (10 h) 3. Calcination: 800°C (24 h)	Ionic compound: LiPF ₆ Solvent: 1:1 • ethylene carbonate • dimethyl carbonate	Li ₄ Ti ₅ O ₁₂	0.425 0.850 2.125 4.250	131.2 101 93.4 84.2	2012	[51]
Flux reaction	MnCl ₂ CoCl ₂ LiOH·H ₂ O	1. Homogenisation: 25°C (NA) 2. Flux reaction: 750°C (48 h)	Ionic compound: LiPF ₆ Solvent: 1:1 • ethylene carbonate • diethyl carbonate	Li	0.028	107	2016	[59]
Flux reaction	CoSO ₄ ·7H ₂ O MnSO ₄ ·H ₂ O C ₂ H ₅ OH H ₂ O NH ₄ HCO ₃ LiOH·H ₂ O	1. Homogenisation: 25°C (3 h) 2. Flux reaction: 800°C (20 h) 3. Rinsing	Ionic compound: LiPF ₆ Solvent: 1:1:1 • ethylene carbonate • dimethyl carbonate • ethyl methyl carbonate	Li	N/A	115.5	2014	[65]
Hydrothermal reaction	MnSO ₄ ·H ₂ O CoSO ₄ ·H ₂ O (NH ₄) ₂ S ₂ O ₈	1. Hydrothermal reaction: 220°C (22 h) 2. Dehydration: 120°C (24 h) 3. Heat treatment: 550°C to 750°C (NA)	Ionic compound: LiPF ₆ Solvent: 1:1 • ethylene carbonate • dimethyl carbonate	Li	0.35	91.6	2016	[61]

Meanwhile, relatively weak electrochemical activity was still notable at 3.9 V (vs. Li⁰ | Li⁺) vicinity attributed by the oxidation and reduction of Mn^{3+/4+} ions [52]. Empirical findings from Windmüller *et al* and Liu *et al* proven that the substitution of fluorine for oxygen loss effectively enhanced the discharge capacity by up to 18% where 128.1 mAh·g⁻¹ attained by LiCoMnO_{3.9}F_{0.1} [67].

Whilst all the three formulated LiCoMnO₄ derivatives exhibit deterioration especially in term of specific discharge capacity, capacity retention as well as coulombic efficiency over cycle, the addition of fluorine tends to flatten the curves and effective in curtailing degradation rate [52]. Besides, it was also suggested that fluorination could potentially improve the specific capacity and cycling stability of lithium cobalt manganese tetroxide cathode [52].

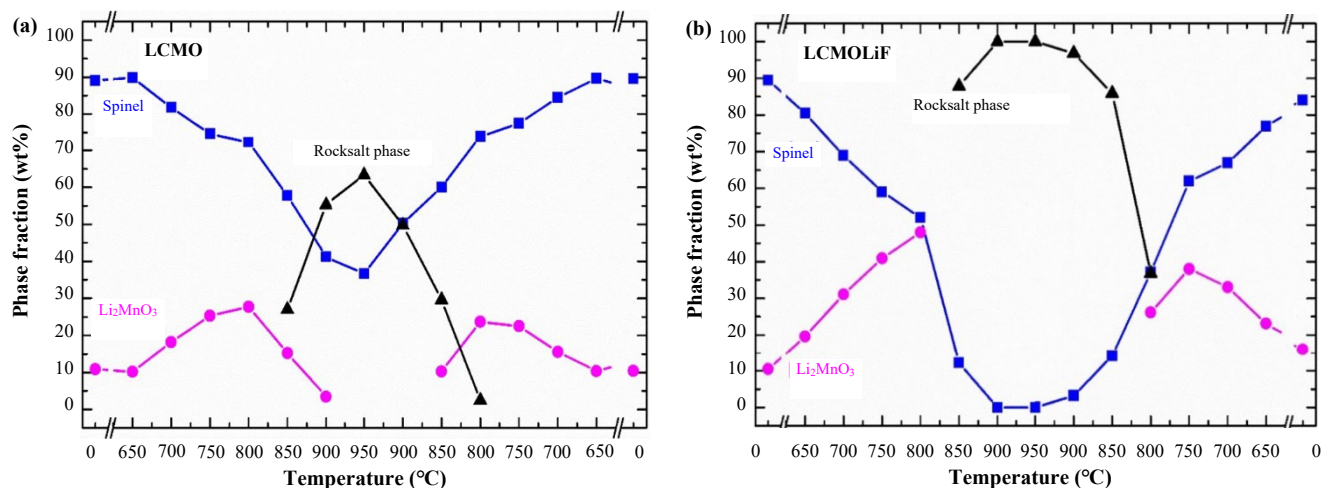


Figure 8. Phases Quantification of (a) LiCoMnO_4 , and (b) LiCoMnO_4 with LiF additive [69] Copyright permission for reuse obtained from publisher via license: 5398780138554.

Similarly it was suggested the reaction temperature for the synthesis of LiCoMnO_4 compound shall ideally be kept as low as necessary to promote the formation of spinel-rich phase even with the presence of fluorine additive as indicated by Figure 8 [69]. Rietveld refinement analysis suggested that the spinel phase LiCoMnO_4 gradually diminished with the increment of reaction temperature due to formation of Li_2MnO_3 (between 600°C to 800°C) and LiCoMnO_3 (between 800°C to 950°C) detected from x-ray diffraction (XRD) with on-site heating [69].

The peak intensity detected on Li_2MnO_3 and LiCoMnO_3 which formed at high temperature gradually declined, while the fraction of spinel phase LiCoMnO_4 increased as the compound were subjected to cooling rate of $5 \text{ K}\cdot\text{min}^{-1}$ [69]. Nevertheless, the experiment only evaluated temperature range between 600°C to 950°C , future research could emphasise on reaction temperature of 500°C to 600°C or lower where 100% of spinel phase may be potentially attained.

5. Conclusion

Spinel structured LiCoMnO_4 which exhibit inherently high reduction potential could prospectively be developed into practical cathode for next generation lithium-ion batteries with attributes such as voltage output and energy density enhanced especially with the breakthrough of solid-state ionic conductor or liquidus electrolyte with high chemical and thermodynamic stability in the near future [54,70,71]. Moreover, LiCoMnO_4 cathode could also be potentially paired with lithium titanate anode instead of conventional graphite or lithium to harvest the benefits of fast charging capability yet without compromising on the energy density and safety of the electrochemical system in complete cell format [44].

Based on fairly limited number of scientific literatures relevant to lithium cobalt manganese tetroxide (LiCoMnO_4) published up to date, it can be summarised that the compound can be synthesised via various techniques, ranging from solid-state reaction to sol-gel synthesis, flux method, and hydrothermal reaction. Solid state reaction was perceived as one of the facile, cost-effective and well-established methods for the synthesis of LiCoMnO_4 . The synthesis approach

however requires high reaction temperature between 800°C to 900°C with prolonged processing duration.

It can be observed that flux method requires slightly lower reaction temperature between 750°C to 800°C with comparatively shorter synthesis duration. The synthesis of LiCoMnO_4 via sol-gel approach on the other hand requires reaction temperature of approximately 380°C , while closed system hydrothermal method with high vapour pressure can be performed at 220°C or lower depending on the solubility limits of precursors selected.

It can be surmised based on limited research findings available up to date that high reaction temperature is not favourable for the synthesis of LiCoMnO_4 and shall be avoided whenever possible. Experimental settings such as precursors used, anodes, electrolytes as well as test variables between independent investigations shall be standardised or normalised whether possible in order to gain full insights on the relationship between synthesis techniques and the performance of LiCoMnO_4 . In cases when oxygen losses is unavoidable, optimal amount of fluoride additives may be introduced to as substitute to fill up oxygen vacancies to yield single phase spinel structured $\text{LiCoMnO}_{(x-y)}\text{F}_{(y)}$ that potentially display single voltage plateau at 5.3 V vicinity and discharge capacity close to $145 \text{ mAh}\cdot\text{g}^{-1}$.

Acknowledgements

This work was funded by the Ministry of Higher Education, Malaysia under Fundamental Research Grant Scheme (FRGS/1/2018/TK03/UTM/02/18).

References

- [1] H. Orru, K. L. Ebi, and B. Forsberg, "The Interplay of Climate Change and Air Pollution on Health," *Current Environmental Health Reports*, vol. 4, no. 4, pp. 504-513, December 01 2017.
- [2] E. E. van der Wall, "Air pollution: 6.6 million premature deaths in 2050!," *Netherlands Heart Journal*, journal article vol. 23, no. 12, pp. 557-558, December 01 2015.

- [3] C. K. Gately, L. R. Hutyra, S. Peterson, and I. Sue Wing, "Urban emissions hotspots: Quantifying vehicle congestion and air pollution using mobile phone GPS data," *Environ Pollut*, vol. 229, pp. 496-504, Oct 2017.
- [4] P. Arévalo-Cid, P. Dias, A. Mendes, and J. Azevedo, "Redox flow batteries: a new frontier on energy storage," *Sustainable Energy & Fuels*, vol. 5, no. 21, pp. 5366-5419, 2021.
- [5] N. F. Attia and K. E. Geckeler, "Polyaniline as a material for hydrogen storage applications," *Macromolecular Rapid Communication*, vol. 34, no. 13, pp. 1043-55, Jul 12 2013.
- [6] N. F. Attia, M. Jung, J. Park, S.-Y. Cho, and H. Oh, "Facile synthesis of hybrid porous composites and its porous carbon for enhanced H₂ and CH₄ storage," *International Journal of Hydrogen Energy*, vol. 45, no. 57, pp. 32797-32807, 2020.
- [7] N. F. Attia, M. Jung, J. Park, H. Jang, K. Lee, and H. Oh, "Flexible nanoporous activated carbon cloth for achieving high H₂, CH₄, and CO₂ storage capacities and selective CO₂/CH₄ separation," *Chemical Engineering Journal*, vol. 379, 2020.
- [8] Y. Deng, C. Eames, B. Fleutot, R. David, J-N. Chotard, E. Suard, C. Masquelier, and M. S. Islam, "Enhancing the Lithium Ion Conductivity in Lithium Superionic Conductor (LISICON) Solid Electrolytes through a Mixed Polyanion Effect," *ACS Applied Materials & Interfaces*, vol. 9, no. 8, pp. 7050-7058, Mar 1 2017.
- [9] W. G. El-Sayed, N. F. Attia, I. Ismail, M. El-Khayat, M. Nogami, and M. S. A. Abdel-Mottaleb, "Innovative and cost-effective nanodiamond based molten salt nanocomposite as efficient heat transfer fluid and thermal energy storage media," *Renewable Energy*, vol. 177, pp. 596-602, 2021.
- [10] M. Jung, J. Park, K. Lee, N. F. Attia, and H. Oh, "Effective synthesis route of renewable nanoporous carbon adsorbent for high energy gas storage and CO₂/N₂ selectivity," *Renewable Energy*, vol. 161, pp. 30-42, 2020.
- [11] H. Lee, V. S. Kumbhar, J. Lee, Y. Choi, and K. Lee, "Highly reversible crystal transformation of anodized porous V₂O₅ nanostructures for wide potential window high-performance supercapacitors," *Electrochimica Acta*, vol. 334, 2020.
- [12] J. Park, S. Y. Cho, M. Jung, K. Lee, Y-C. Nah, N. F. Attia, and H. Oh, "Efficient synthetic approach for nanoporous adsorbents capable of pre- and post-combustion CO₂ capture and selective gas separation," *Journal of CO₂ Utilization*, vol. 45, 2021.
- [13] J. Park, M. Jung, H. Jang, K. Lee, N. F. Attia, and H. Oh, "A facile synthesis tool of nanoporous carbon for promising H₂, CO₂, and CH₄ sorption capacity and selective gas separation," *Journal of Materials Chemistry A*, vol. 6, no. 45, pp. 23087-23100, 2018.
- [14] B. Singh, B. Singh, Z. Wang, S. Park, G. S. Gautam, J-N. Chotard, L. Croguennec, D. Carlier, A. K. Cheetham, C. Masquelier, and P. Canepa, "A chemical map of NaSICON electrode materials for sodium-ion batteries," *Journal of Materials Chemistry A*, vol. 9, no. 1, pp. 281-292, 2021.
- [15] V. Etacheri, R. Marom, R. Elazari, G. Salitra, and D. Aurbach, "Challenges in the development of advanced Li-ion batteries: a review," *Energy & Environmental Science*, vol. 4, no. 9, 2011.
- [16] Y. Yang, Z. Tan, and Y. Ren, "Research on factors that influence the fast charging behavior of private battery electric vehicles," *Sustainability*, vol. 12, no. 8, 2020.
- [17] C. M. Hayner, X. Zhao, and H. H. Kung, "Materials for rechargeable lithium-ion batteries," *Annual Review of Chemical and Biomolecular Engineering*, vol. 3, pp. 445-471, 2012.
- [18] M. Root, *The TAB Battery Book: An In-Depth Guide to Construction, Design, and Use*. McGraw-Hill Education, 2010.
- [19] R. Schmuck, R. Wagner, G. Hörpel, T. Placke, and M. Winter, "Performance and cost of materials for lithium-based rechargeable automotive batteries," *Nature Energy*, vol. 3, no. 4, pp. 267-278, 2018.
- [20] J. Gao, S.-Q. Shi, and H. Li, "Brief overview of electrochemical potential in lithium ion batteries," *Chinese Physics B*, vol. 25, no. 1, 2016.
- [21] P. Krivik and P. Bac, "Electrochemical Energy Storage," in *Energy Storage - Technologies and Applications*, 2013.
- [22] C. Liu, Z. G. Neale, and G. Cao, "Understanding electrochemical potentials of cathode materials in rechargeable batteries," *Materials Today*, vol. 19, no. 2, pp. 109-123, 2016.
- [23] C. Julien, A. Mauger, K. Zaghib, and H. Groult, "Optimization of Layered Cathode Materials for Lithium-Ion Batteries," *Materials*, vol. 9, no. 7, Jul 19 2016.
- [24] R. Tatara, P. Karayaylali, Y. Yu, Y. Zhang, L. Giordano, F. Maglia, R. Jung, J. P. Schmidt, I. Lund, and Y. Shao-Horn, "The Effect of Electrode-Electrolyte Interface on the Electrochemical Impedance Spectra for Positive Electrode in Li-Ion Battery," *Journal of The Electrochemical Society*, vol. 166, no. 3, pp. A5090-A5098, 2018.
- [25] M. Osiak, H. Geaney, E. Armstrong, and C. O' Dwyer, "Structuring materials for lithium-ion batteries: advancements in nanomaterial structure, composition, and defined assembly on cell performance," *Journal of Materials Chemistry A*, vol. 2, no. 25, 2014.
- [26] C. Julien, A. Mauger, A. Vijn, and K. Zaghib, *Lithium Batteries: Science and Technology*. Springer International Publishing, 2015, p. 51.
- [27] K. N. Wood, E. Kazyak, A. F. Chadwick, K-H. Chen, J-G. Zhang, K. Thornton, and N. P. Dasgupta, "Dendrites and pits: Untangling the complex behavior of lithium metal anodes through operando video microscopy," *ACS Central Science*, vol. 2, no. 11, pp. 790-801, Nov 23 2016.
- [28] R. Zhu, J. Feng, and Z. Guo, "In situ observation of dendrite behavior of electrode in half and full cells," *Journal of The Electrochemical Society*, vol. 166, no. 6, pp. A1107-A1113, 2019.
- [29] J. B. Quinn, T. Waldmann, K. Richter, M. Kasper, and M. Wohlfahrt-Mehrens, "Energy density of cylindrical li-ion cells: A comparison of commercial 18650 to the 21700 cells," *Journal of The Electrochemical Society*, vol. 165, no. 14, pp. A3284-A3291, 2018.
- [30] C. Sun, "Batteries & Fuel Cells" *Advanced Battery Materials*. Wiley, 2019.

- [31] X. Hu, Y. Zheng, D. A. Howey, H. Perez, A. Foley, and M. Pecht, "Battery warm-up methodologies at subzero temperatures for automotive applications: Recent advances and perspectives," *Progress in Energy and Combustion Science*, vol. 77, 2020.
- [32] A. Tomaszewska, Z. Chu, X. Feng, S. O'Kane, X. Liu, J. Chen C. Ji, E. Endler, R. Li, L. Liu, Y. Li, S. Zheng, S. Vetterlein, M. Gao, J. Du, M. Parkes, M. Ouyang, M. Marinescu, and B. Wu, "Lithium-ion battery fast charging: A review," *eTransportation*, vol. 1, 2019.
- [33] S. Chauque, F. Y. Oliva, A. Visintin, D. Barraco, E. P. M. Leiva, and O. R. Cámara, "Lithium titanate as anode material for lithium ion batteries: Synthesis, post-treatment and its electrochemical response," *Journal of Electroanalytical Chemistry*, vol. 799, pp. 142-155, 2017.
- [34] J. Christensen, V. Srinivasan, and J. Newman, "Optimization of lithium titanate electrodes for high-power cells," *Journal of The Electrochemical Society*, vol. 153, no. 3, 2006.
- [35] R. Fu, X. Zhou, H. Fan, D. Blaisdell, A. Jagadale, X. Zhang, and R. Xiong, "Comparison of lithium-ion anode materials using an experimentally verified physics-based electrochemical model," *Energies*, vol. 10, no. 12, 2017.
- [36] H. Zhao, "Lithium titanate-based anode materials," in *Rechargeable Batteries* (Green Energy and Technology, 2015, pp. 157-187.
- [37] M. S. Whittingham, "Lithium batteries and cathode materials," *Chemical Reviews*, vol. 104, no. 10, pp. 4271-4302, 2004.
- [38] N. Van Hiep, and K. Young Ho, "Recent advances in cathode and anode materials for lithium ion batteries," *Applied Chemistry for Engineering*, vol. 29, no. 6, pp. 635-644, 2018.
- [39] E. A. Suslov, O. V. Bushkova, E. A. Sherstobitova, O. G. Reznitskikh, and A. N. Titov, "Lithium intercalation into TiS_2 cathode material: phase equilibria in a Li-TiS_2 system," *Ionics*, vol. 22, no. 4, pp. 503-514, 2015.
- [40] S. Fang, D. Bresser, and S. Passerini, "Transition metal oxide anodes for electrochemical energy storage in lithium- and sodium-ion batteries," *Advanced Energy Materials*, vol. 10, no. 1, 2019.
- [41] M. A. Kebede, and F. I. Ezema, *Electrochemical Devices for Energy Storage Applications*. CRC Press, 2019.
- [42] H. R. Shaari and V. Sethuprakash, "Review of Electrochemical performance of LiNiO_2 and their derivatives as cathode material for lithium-ion batteries," *Jurnal Teknologi*, vol. 70, no. 1, 2014.
- [43] P. Kalyani, and N. Kalaiselvi, "Various aspects of LiNiO_2 chemistry: A review," *Science and Technology of Advanced Materials*, vol. 6, no. 6, pp. 689-703, 2005.
- [44] Y. C. Lyu, J. Huang, and H. Li, "Layered and spinel structural cathodes," in *Rechargeable Batteries*, 2015, pp. 67-92.
- [45] Z. Liu, A. Yu, and J. Y. Lee, "Synthesis and characterization of $\text{LiNi}_{1-x-y}\text{Co}_x\text{Mn}_y\text{O}_2$ as the cathode materials of secondary lithium batteries," *Journal of Power Sources*, vol. 81-82, pp. 416-419, 1999.
- [46] F. Schipper, E. M. Erickson, C. Erk, J.-Y. Shin, F. F. Chesneau, and D. Aurbach, "Review—recent advances and remaining challenges for lithium ion battery cathodes," *Journal of The Electrochemical Society*, vol. 164, no. 1, pp. A6220-A6228, 2016.
- [47] Q. Zhen, S. Bashir, and J. L. Liu, *Nanostructured Materials for Next-Generation Energy Storage and Conversion: Advanced Battery and Supercapacitors*. Springer Berlin Heidelberg, 2019.
- [48] X. Sun, Z. Li, X. Wang, and C. Li, "Technology development of electric vehicles: A review," *Energies*, vol. 13, no. 1, 2019.
- [49] F. Zhou, M. Cococcioni, K. Kang, and G. Ceder, "The Li intercalation potential of LiMPO_4 and LiMSiO_4 olivines with $\text{M}=\text{Fe, Mn, Co, Ni}$," *Electrochemistry Communications*, vol. 6, no. 11, pp. 1144-1148, 2004.
- [50] N. Reeves-McLaren, M. Hong, H. Alqurashi, L. Xue, J. Sharp, A. J. Rennie, and R. Boston "The Spinel LiCoMnO_4 : 5V cathode and conversion anode," *Energy Procedia*, vol. 151, pp. 158-162, 2018.
- [51] X. Huang, M. Lin, Q. Tong, X. Li, Y. Ruan, and Y. Yang, "Synthesis of LiCoMnO_4 via a sol-gel method and its application in high power $\text{LiCoMnO}_4/\text{Li}_4\text{Ti}_5\text{O}_{12}$ lithium-ion batteries," *Journal of Power Sources*, vol. 202, pp. 352-356, 2012.
- [52] A. Windmüller, C.-L. Tsai, S. Moller, M. Baski, Y. J. Sohn, S. Uhlenbruck, and O. Guillon, "Enhancing the performance of high-voltage LiCoMnO_4 spinel electrodes by fluorination," *Journal of Power Sources*, vol. 341, pp. 122-129, 2017.
- [53] K. Ariyoshi, H. Yamamoto, and Y. Yamada, "High dimensional stability of LiCoMnO_4 as positive electrodes operating at high voltage for lithium-ion batteries with a long cycle life," *Electrochimica Acta*, vol. 260, pp. 498-503, 2018.
- [54] X. Fan, X. Ji, L. Chen, J. Chen, T. Deng, F. Han, J. Yue, N. Piao, R. Wang, X. Zhou, X. Xiao, L. Chen, and C. Wang, "All-temperature batteries enabled by fluorinated electrolytes with non-polar solvents," *Nature Energy*, vol. 4, no. 10, pp. 882-890, 2019.
- [55] T.-F. Yi, S.-Y. Yang, and Y. Xie, "Recent advances of $\text{Li}_4\text{Ti}_5\text{O}_{12}$ as a promising next generation anode material for high power lithium-ion batteries," *Journal of Materials Chemistry A*, vol. 3, no. 11, pp. 5750-5777, 2015.
- [56] H. Kawai, M. Nagata, H. Kageyama, H. Tukamoto, and A. R. West, "5 V lithium cathodes based on spinel solid solutions $\text{Li}_2\text{Co}^{1+}\text{XMn}^{3-x}\text{O}_8$: $-1 \leq x \leq 1$," *Electrochimica Acta*, vol. 45, no. 1, pp. 315-327, 1999.
- [57] H. Kawai, M. Nagata, H. Tukamoto, and A. R. West, "A new lithium cathode LiCoMnO : Toward practical 5 V lithium batteries," *Electrochemical and Solid-State Letters*, vol. 1, no. 5, 1999.
- [58] N. Kuwata, S. Kudo, Y. Matsuda, and J. Kawamura, "Fabrication of thin-film lithium batteries with 5-V-class LiCoMnO_4 cathodes," *Solid State Ionics*, vol. 262, pp. 165-169, 2014.
- [59] Y. Hamada, N. Hamao, K. Kataoka, N. Ishida, Y. Idemoto, and J. Akimoto, "Single crystal synthesis, crystal structure and electrochemical property of spinel-type LiCoMnO_4 as 5 V positive electrode materials," *Journal of the Ceramic Society of Japan*, vol. 124, no. 6, pp. 706-709, 2016.
- [60] C. M. Julien and A. Mauger, "Review of 5-V electrodes for Li-ion batteries: status and trends," *Ionics*, vol. 19, no. 7, pp. 951-988, 2013.

- [61] M. You, X. Huang, M. Lin, Q. Tong, X. Li, Y. Ruan, and Y. Yang, "Preparation of LiCoMnO_4 assisted by hydrothermal approach and its electrochemical performance," *American Journal of Engineering and Applied Sciences*, vol. 9, no. 2, pp. 396-405, 2016.
- [62] E. McCalla, *Consequences of Combinatorial Studies of Positive Electrodes for Li-ion Batteries*. Springer International Publishing, 2014.
- [63] D. Pasero, S. de Souza, N. Reeves, and A. R. West, "Oxygen content and electrochemical activity of $\text{LiCoMnO}_{4-\delta}$," *Journal of Materials Chemistry*, vol. 15, no. 41, 2005.
- [64] K. Ariyoshi, H. Yamamoto, and Y. Yamada, "Synthesis optimization of electrochemically active LiCoMnO_4 for high-voltage lithium-ion batteries," *Energy & Fuels*, vol. 35, no. 16, pp. 13449-13456, 2021.
- [65] M. Hu, Y. Tian, J. Wei, D. Wang, and Z. Zhou, "Porous hollow LiCoMnO_4 microspheres as cathode materials for 5 V lithium ion batteries," *Journal of Power Sources*, vol. 247, pp. 794-798, 2014.
- [66] A. Windmüller, "Synthesis and analysis of spinel cathode materials for high voltage solid-state lithium batteries," PhD, Institut für Energie- und Klimaforschung, RWTH Aachen University, 2018.
- [67] S. Liu, H. He, and C. Chang, "Understanding the improvement of fluorination in 5.3 V LiCoMnO_4 spinel," *Journal of Alloys and Compounds*, vol. 860, 2021.
- [68] A. Windmüller, C. A. Bridges, C-L. Tsai, S. Lobe, C. Dellen, G. M. Veith, M. Finsterbusch, S. Uhlenbruck, and O. Guillon, "Impact of fluorination on phase stability, crystal chemistry, and capacity of LiCoMnO_4 high voltage spinels," *ACS Applied Energy Materials*, vol. 1, no. 2, pp. 715-724, 2018.
- [69] A. Windmüller, C. Dellen, S. Lobe, C-L. Tsai, S. Moller, Y. J. Sohn, N. Wettengl, M. Finsterbusch, S. Uhlenbruck, and O. Guillon, "Thermal stability of 5 V LiCoMnO_4 spinels with LiF additive," *Solid State Ionics*, vol. 320, pp. 378-386, 2018.
- [70] C. Zhang, "High-voltage electrolytes," *Nature Energy*, vol. 4, no. 5, pp. 350-350, 2019.
- [71] L. Chen, X. Fan, E. Hu, X. Ji, j. Chen, S. Hou, T. Deng, J. Li, D. Su, X. Yang, and C. Wang "Achieving high energy density through increasing the output voltage: A highly reversible 5.3 V Battery," *Chem*, vol. 5, no. 4, pp. 896-912, 2019.